ELSEVIER

Physics of the Earth and Planetary Interiors 85 (1994) 155–171

PHYSICS OF THE EARTH AND PLANETARY INTERIORS

Fuzzy *c*-means cluster analysis of early diagenetic effects on natural remanent magnetisation acquisition in a 1.1 Myr piston core from the Central Mediterranean

M.J. Dekkers [a,*], C.G. Langereis [a], S.P. Vriend [b], P.J.M. van Santvoort [b], G.J. de Lange [b]

[a] *Paleomagnetic Laboratory 'Fort Hoofddijk', Department of Geophysics, Institute of Earth Sciences, Utrecht University, Budapestlaan 17, 3584 CD Utrecht, Netherlands*

[b] *Department of Geochemistry, Institute of Earth Sciences, Utrecht University, Budapestlaan 4, 3584 CD Utrecht, Netherlands*

Received 24 September 1993; revision accepted 28 January 1994

Abstract

The influence of early diagenesis on the natural remanent magnetisation (NRM) in sediments from the Calabrian ridge (Central Mediterranean) is analysed with the help of fuzzy *c*-means (FCM) cluster analysis and non-linear mapping (NLM). The sediments are variably coloured: white, beige, purplish, greenish and grey layers occur with occasionally intercalated sapropels. The NRM acquired depends on both depositional conditions and diagenetic processes. To describe these, FCM was performed with χ_{in}, ARM, $CaCO_3$, Ba, Mn and S as variables. An eight-cluster model was derived with the clusters belonging to two categories: one expressing mainly diagenetic processes, i.e. dissolution and precipitation, and the other expressing mainly depositional conditions. The impact of diagenesis on NRM acquisition is profound and not restricted to the close vicinity of the anoxic sapropelitic layers. As a consequence, the influence of diagenetic processes on the NRM should be thoroughly assessed when selecting samples, e.g. for the determination of the relative palaeointensity of the geomagnetic field. Application of multivariate classification techniques appears to be useful because it links rock magnetic parameters to the geochemical environment. In the present piston core, three short reversed geomagnetic events in the Brunhes chron are preserved and, indeed, occur in clusters expressing no or minor diagenesis. The recording of the Blake event, however, has been prevented by later precipitation of magnetite in the corresponding interval.

1. Introduction

A recent palaeomagnetic study of a 37 m long piston core (KC-01B) from the Calabrian ridge in the Central Mediterranean (36°15′25″N, 17°44′34″E) revealed a continuous section from Recent to below the Jaramillo subchron (Langereis et al., 1994; see Fig. 1). Core KC-01B contains the oldest sapropelitic layers recorded in a piston core so far and considerably narrows the gap between piston cores and land sections (e.g. Hilgen, 1991). The presence of sapropelitic layers allows a very precise chronological framework by correlating

* Corresponding author.

SSDI 0031-9201(94)05054-2

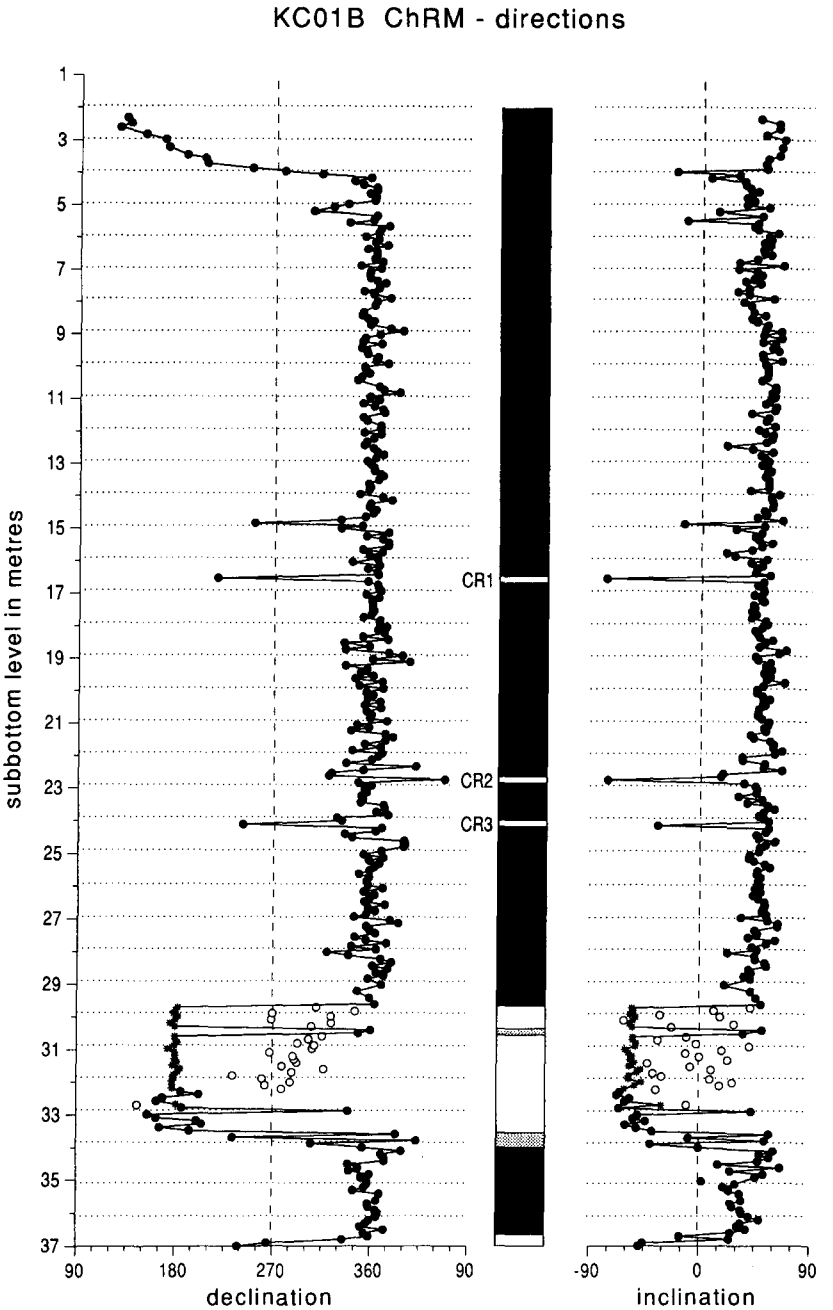

Fig. 1. Directions of the characteristic remanent magnetisation for the KC-01B core as a function of subbottom level. Full symbols refer to stable end point directions as determined from Zijderveld plots, while open symbols refer to less well-defined directions; corresponding great circle analyses are indicated with asterisks. The polarity of the shaded parts is uncertain. Three short reversed geomagnetic events in the Brunhes are labelled as CR1, CR2 and CR3.

these layers to the insolation curve (Langereis et al., 1994), which is dominated by the precessional cycle of the Earth's orbit.

Furthermore, three short reversed geomagnetic events in the Brunhes chron — CR1, CR2 and CR3 — (CR stands for Calabrian ridge) could be dated at 319 ± 2, 497 ± 2 and 552 ± 2 ka (Langereis et al., 1994). In Fig. 1, these reversed periods are shown as single-sample events but detailed resampling of these zones has confirmed their existence. These accurate ages allow events that are temporally closely spaced in time to be distinguished and solve one of the problems put forward by, e.g. Løvlie (1989): are we dealing with one and the same event or with more than one when correlating different records.

The most important problem, however, is how well actual events are being preserved in the sedimentary column. If the sediments studied here would have been perfect recorders of the geomagnetic field, more reversed geomagnetic events should have been detected (cf. Champion et al., 1988). The study by Langereis et al. (1994) shows the absence of the Blake event, despite detailed resampling of the corresponding interval, between sapropels S4 and S5 (Fig. 2). Its existence, between these sapropelitic layers is well established in the Mediterranean (Ryan, 1972; Tucholka et al., 1987; Tric et al., 1991). The absence of the Blake event suggests that (early) diagenetic phenomena occurred in sediments of core KC-01B, complicating the acquisition process of the natural remanent magnetisation (NRM) and its interpretation. Recognition of diagenetic zones is furthermore important for establishing meaningful relative palaeointensity records. Rock magnetic selection criteria and techniques to obtain such records were recently reviewed by Tauxe (1993). Work by Karlin (1990a, b) and Leslie et al. (1990) shows that dissolution

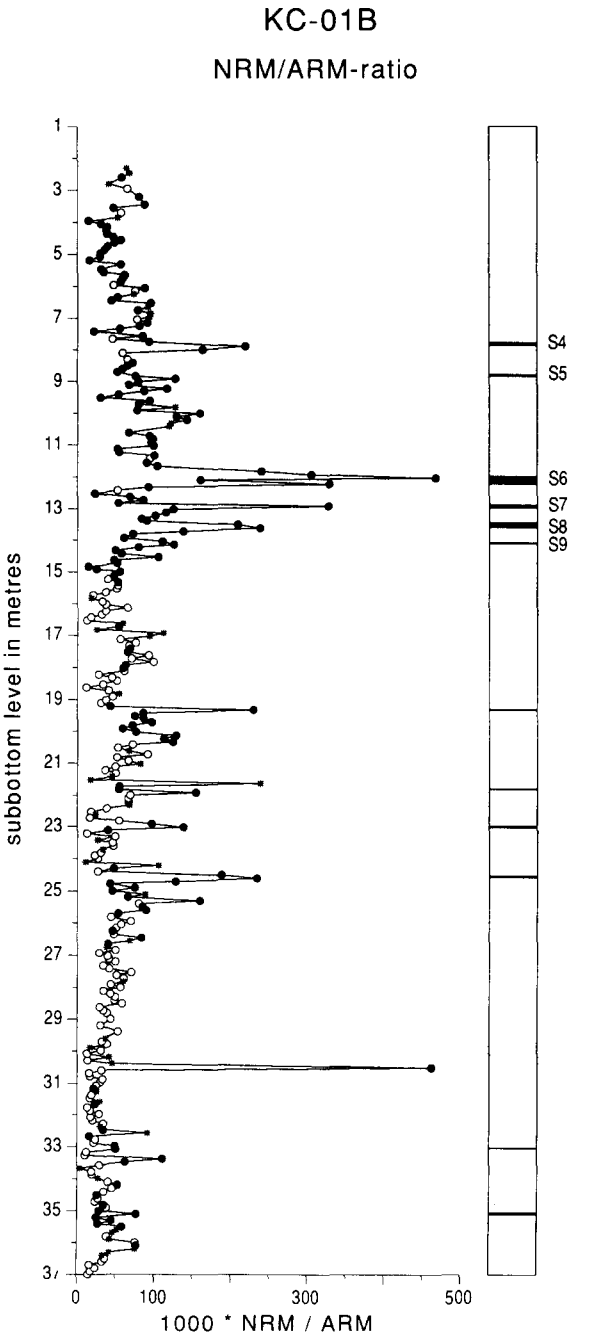

Fig. 2. The NRM/ARM ratio as a function of depth. Open circles denote samples where no diagenesis is suspected based on multivariate statistical techniques as outlined in the present work. Star symbols refer to samples with a deviating ARM/χ_{in} value. Samples which are influenced by diagenetic processes are shown in full circles. Note the high NRM/ARM values in the vicinity of the sapropelitic layers, indicated in black in the simplified lithological column. Sapropels S4–S9 are numbered according to the Mediterranean sapropelitic layer index.

of magnetic carriers is common in suboxic and anoxic sedimentary environments. Early diagenetic processes like dissolution and precipitation of iron (hydr)oxides may influence strongly the NRM acquisition process. The finest oxide particles are preferentially dissolved (Karlin, 1990a, b; Leslie et al., 1990), while precipitation of iron oxides will lead to the formation of a chemical remanent magnetisation (CRM). This disturbs the (relative) palaeointensity record because:

(1) preferential dissolution biases normalisation parameters, especially the anhysteretic remanent magnetisation (ARM);

(2) CRM is a NRM acquisition mechanism quite different from postdepositional remanent magnetisation (pDRM);

(3) a CRM represents a different (younger, and less constrained) acquisition time (e.g. Van Hoof et al., 1993).

To illustrate that these processes can be significant, the NRM/ARM ratio vs. subbottom depth of core KC-01B is shown in Fig. 2. It shows conspicuously high values close to sapropelitic layers where diagenetic phenomena are widespread (Van Os et al., 1993), hence intuitively casting doubt on the geomagnetic significance of this ratio, at least in (near-)sapropelitic intervals. In land sections, the additional influence of recent weathering may be subtle but can be considerable (Van Velzen, 1993), but sediments from marine cores generally do not suffer from recent (subaerial) weathering. Hence, they are suited to study the impact of early diagenetic processes. The KC-01B piston core provides a variety of sedimentary and diagenetic regimes which enables a study of their combined effect.

The NRM intensity is the result of geomagnetic field intensity and magnetomineralogy, which in turn depends on depositional and diagenetic processes that may vary between (and even within) lithological subunits. Our approach in determining the influence of diagenesis consists of measuring various magnetic and geochemical parameters for each sample. Subsequently, we apply multivariate statistical techniques for the recognition of groups within the data set. Within each group or cluster, the samples (or cases) have similar magnetic and geochemical characteristics and, consequently, dominant processes that have acted upon each group can be detected. For this study, we have used the following magnetic and chemical variables: ARM, the initial magnetic susceptibility (χ_{in}), $CaCO_3$, S, Mn and Ba. We use fuzzy *c*-means (FCM) cluster analysis, a multivariate statistical technique requiring no a priori knowledge, to designate groups with similar characteristics.

2. Lithology, depositional conditions and diagenesis

The sediments of the piston core consist of an alternation of grey, greenish, olive-coloured, yellowish, white and beige shades, rather similar to the lithology of the Pliocene Trubi and Narbone marl formations in southern Italy and Sicily (e.g. Hilgen, 1991). The olive-greenish coloured layers represent probably intermediate conditions between the grey and beige layers. The sapropelitic layers are black. Although they are similar in lithology, the average carbonate content of the sediments from KC-01B (20–65%) is lower than that of the Trubi marls (55–70%; Hilgen and Langereis, 1989). The sediments represent various depositional conditions, from oxic–suboxic (beige and white) through suboxic–anoxic (grey) to anoxic (sapropelitic layers) (cf. Froelich et al., 1979; Lyle, 1983; de Lange, 1986).

Diagenesis may be described as the sum of postdepositional changes of sediments as a result of interacting physical, chemical and biological processes. One of the more important processes is the bacterial degradation of organic material whereby successively oxygen, nitrate, manganese and iron (oxyhydr)oxides and sulphate are used as terminal electron acceptors. The use of manganese- and iron (oxyhydr)oxides by bacteria leads to dissolution of these minerals. Subsequently, the mobile divalent iron and manganese ions diffuse through the sediment. They will precipitate again as oxyhydroxides under more oxic conditions. Under anoxic conditions, iron can react with sulphide to form pyrite.

In oxic and suboxic conditions, bacterially mediated magnetite production occurs (Karlin and

Levi, 1985), and may even occur in anoxic conditions (Sakaguchi et al., 1993). In anoxic conditions, Canfield and Berner (1987) showed that magnetite dissolution may occur. This occurs only after titration of more reactive iron-bearing phases, like adsorbed iron and goethite or lepidocrocite (Canfield, 1989; Leslie et al., 1990). Magnetite may resist microbial reduction (Lovley and Phillips, 1986; Lovley et al., 1987). The preservation of magnetic intermediate phases in the sulphate reduction chain, greigite and pyrrhotite, is probably not widespread because of the wide availability of marine sulphate. High χ_{in} values which could be taken as indication for these magnetic phases, are not observed in sapropelitic layers. Thermomagnetic analyses (Fig. 3) do not hint at the presence of magnetic sulphides. Barium is a productivity proxy because foraminiferal tests contain $BaSO_4$. During conditions where $[SO_4^{2-}]$ is extremely low, it may become mobile because $BaSO_4$ dissolves (Van Os et al., 1991). It precipitates again where the sulphate concentration is only marginally higher. Barium is therefore an attractive element to trace so-called 'burnt down' sapropelitic layers: the organic material and the high sulphide content have disappeared because of oxidation, but the high barium content still persists.

The lithological cyclicity is induced by astronomically forced variations in seasonal contrast, giving rise to a varying supply of terrigenic (mainly clay minerals) and biogenic material (mainly $CaCO_3$). The lithological variation in turn induces varying redox conditions and these cyclic (palaeo)redox conditions lead to different diagenetic regimes where reductively dissolved species may precipitate again upon meeting more oxidising (or less reducing) conditions. Van Hoof et al. (1993) described formation of secondary magnetite in the Trubi marls under suboxic conditions. In the KC-01B core, the presence of anoxic sapropelitic layers with a high reductive reservoir of organic carbon may lead to even more extreme diagenetic conditions.

3. Variables and statistical methods

Palaeomagnetic samples (8 cm^3 cylinders) were taken from the core at 10 cm intervals, corre-

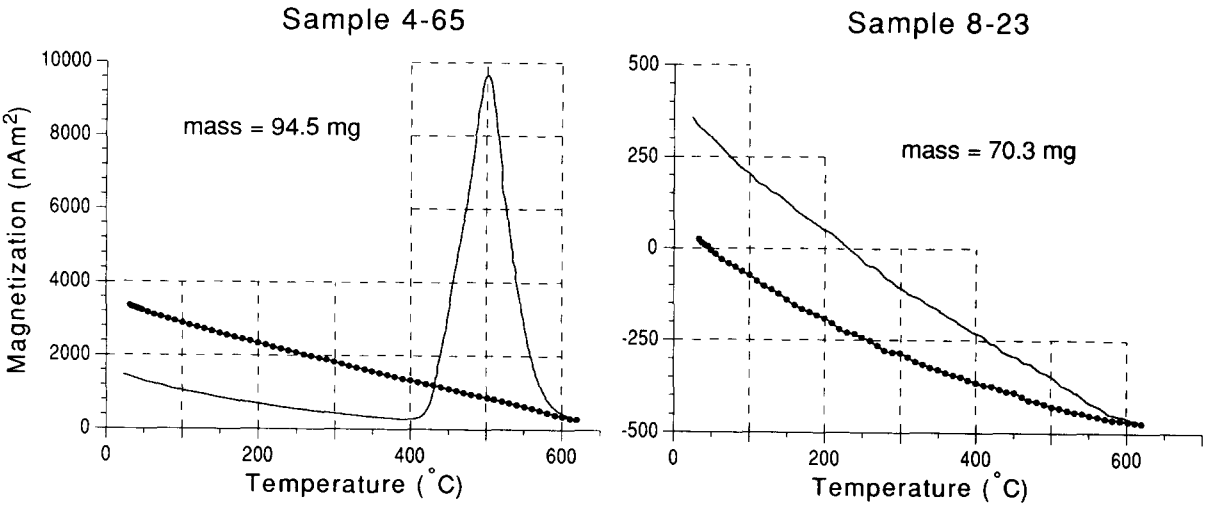

Fig. 3. Thermomagnetic analysis of sample 4-65 (grey lithology) and sample 8-23 (beige lithology). Thermomagnetic analysis was done in air with a high-sensitivity horizontal translation-type Curie balance making use of a sinusoidally cycling applied magnetic field (Mullender et al., 1993); the field was cycled between 200 and 400 mT. The heating rate was 6°C min^{-1} and the cooling rate 10°C min^{-1}. No preconcentration of magnetic material is necessary. The increase in magnetisation in sample 4-65 from 420°C is caused by magnetite formed through breakdown of sulphides, likely pyrite. Sample 8-23 shows a minute discontinuity close to 580°C, suggesting magnetite. No magnetite is produced during thermomagnetic analysis of this sample.

sponding to an average resolution of approximately 3000 years. At the same level, a sample for geochemical analysis was taken. A total of 337 samples was analysed for Ca, Mn, S and Ba while also χ_{in} and ARM were determined to link rock magnetic and chemical parameters.

3.1. Variables

Magnetic variables

The magnetic variables used in the present study are NRM, ARM and χ_{in}. The NRM is taken as the intensity of the NRM after 20 mT AF demagnetisation. It generally varies between 1 and 10 mA m^{-1}; close to sapropelitic layers it is usually one order of magnitude lower. Anhysteretic remanent magnetisation is induced in a 100 mT peak alternating field with a direct field of 29 μT. The ARM intensities vary less than NRM intensities and are in general between 50 and 200 mA m^{-1} (χ_{ARM} of $30-70 \times 10^3$). Only close to sapropelitic layers, the ARM intensity is more than one order of magnitude lower. NRM and ARM intensities were measured with a vertical 2G superconducting magnetometer (model 740-R) or with a digital spinner magnetometer based on the Jelinek JR3 drive unit. Initial susceptibility is measured with a Jelinek KLY-2 susceptibility bridge; it varies between 40 and 400 μSI. These low values indicate a low ferromagnetic contribution. Variation in χ_{in} close to sapropelitic layers is less distinct than variations in NRM and ARM. Because variations in NRM intensity are partly caused by intensity variations of the geomagnetic field, NRM is not included in the FCM cluster analysis which is aimed at the discrimination of diagenesis and lithology.

Chemical variables

Calcium carbonate is used to represent variations in productivity ($CaCO_3$, Van Os et al., 1993). Sulphur, Mn and Ba are included to represent lithology and redox conditions. Manganese is slightly more mobile than iron in suboxic conditions (Froelich et al., 1979) and therefore may serve to recognise precipitation zones in suboxic conditions. High S contents are indicative of anoxic conditions (sulphate reduction, followed by pyrite formation), while high Ba contents (productivity proxy) are closely related to sapropelitic layers where large amounts of organic material have accumulated. Barium peaks often just outside sapropelitic layers which is caused by diagenetic remobilisation in the anoxic sapropelitic layer (Van Os et al., 1991). Calcium carbonate is the Ca concentration recalculated to $CaCO_3$. Calcium, S, Mn and Ba are determined by inductively coupled plasma (ICP) emission spectrography using an ARL34000 instrument. Accuracy and precision were checked with laboratory and international standards, and with replicate analyses. The analytical error (relative percentages) is better than 4% for Ca and better than 7% for S, Mn and Ba.

3.2. Statistical methods: fuzzy c-means cluster analysis and non-linear mapping

In complicated data sets, subtle patterns and considerable compositional overlap may occur. They may go unnoticed if only simple, rather rigid uni- and bivariate statistical techniques are used. Multivariate classification techniques are well suited to discern grouping in such cases. These techniques can be divided into two groups: those requiring a priori knowledge about a classificatory parameter (e.g. discriminant function analysis), and those which do not (e.g. Howarth and Sinding-Larsen, 1983). Clustering techniques do not require a priori knowledge about partitioning. Of these techniques, c-means clustering is aimed at minimising the distance of a case (sample) to its cluster centre. Iteratively, cases are partitioned over a predetermined number of clusters. The inclusion of fuzziness (the concept was introduced by Zadeh (1965)) in c-means clustering thus leads to 'fuzzy c-means (FCM) clustering'. The fuzzy models are aimed at determining the similarity between a case and all clusters rather than forcing a case completely to a specific cluster (Bezdek, 1981). This similarity is expressed in a continuous function (membership) between zero (completely different) and one (identical). Intermediate cases are recognised by significant memberships of more than one cluster. FCM has been shown to facilitate greatly the

interpretation of multivariate data sets expressing gradual trends (e.g. Middelburg and de Lange, 1988; Vriend et al., 1988; Frapporti et al., 1993). For the present data set, the aim was to label clusters meaningfully based upon lithological and dissolution–precipitation criteria. In this way, the diagenetic influence on each sample can be assessed.

A statistical technique to evaluate the FCM clustering is non-linear mapping (NLM). The algorithm was first presented by Sammon (1969, 1970) and has been mainly applied to geochemical data sets (cf. Vriend et al., 1988). Basically, NLM determines a two-dimensional image of a multidimensional data cloud whereby the distortion of the intersample distances is kept at a minimum. The NLM algorithm is different from that used in FCM and NLM assumes no grouping of data in advance. If both techniques show similar data groupings, it is likely that these are meaningful, and the homogeneity of individual clusters can be tested. Before running the FCM and NLM programs all data were logarithmically transformed because histograms revealed log–normal distributions.

4. Results

4.1. Univariate and bivariate statistics

Langereis et al. (1994) found that total sulphur (S) shows maxima in and below sapropelitic layers and that Ba maxima are closely associated with the sapropelitic layers (because of diagenetic mobilisation, see Van Os et al., 1991). The NRM behaviour is reported in Langereis et al. (1994). A next step in the interpretation of the KC-01B data set is the visualisation of possible trends grouped by sediment colour, i.e. a division into oxic–suboxic conditions (beige and white shades) and anoxic conditions (grey and sapropelitic layers). The anhysteretic susceptibility (χ_{ARM}) is plotted vs. χ_{in} in Fig. 4(a). The samples appear to be split into two groups with the grey-coloured samples generally having a lower χ_{ARM} than the beige and white samples. Their χ_{in} decreases distinctly less: an indication that χ_{in} is dominated by the paramagnetic contribution of the clay minerals. This behaviour was interpreted by Bloemendal et al. (1992) as being indicative of reductive dissolution of magnetic carriers. Some grey samples plot in the beige + white area, however, while some plot even above this area. These samples are located close to sapropelitic layers and usually in the direct vicinity of beige layers. Grey-coloured samples generally have a higher S content than the beige- and white-coloured samples (Fig. 4b). The plots of NRM intensity vs. ARM intensity (Fig. 4c) and NRM vs. χ_{ARM}/χ_{in} (Fig. 4d) show that the grey-coloured samples are considerably more dispersed than the beige samples. A number of grey-coloured samples, however, plot in the area of the beige samples. Hence, it is not possible to distinguish the lithology on the basis of these magnetic data alone. The overlap of grey and beige samples indicates that a division based on sediment colour is too rigid. Diagenetic processes, i.e. dissolution and precipitation, seem to occur to a different degree within the same lithology and they are possibly not restricted to a single lithology. A meaningful interpretation is impractical, therefore, if one uses only uni- and bivariate statistics. The gradual nature of diagenesis combined with lithological variation makes fuzzy clustering techniques particularly suitable to discern groups with similar characteristics.

4.2. Derivation and interpretation of the cluster model

Like the number of components in multivariate principal component analysis (Jöreskog et al., 1976), there are no unambiguous rules to determine the number of clusters. Vriend et al. (1988) showed that statistical functionals to describe clustering properties (given by the FCM program) should not be applied too rigidly but should rather be used as guidelines. Each cluster should be reasonably homogeneous and fit in a chemical and rock magnetic context. To derive an adequate model, we interpreted models with an increasing number of clusters. The statistical functionals did not indicate an evident optimal number of clusters. General trends in the data set

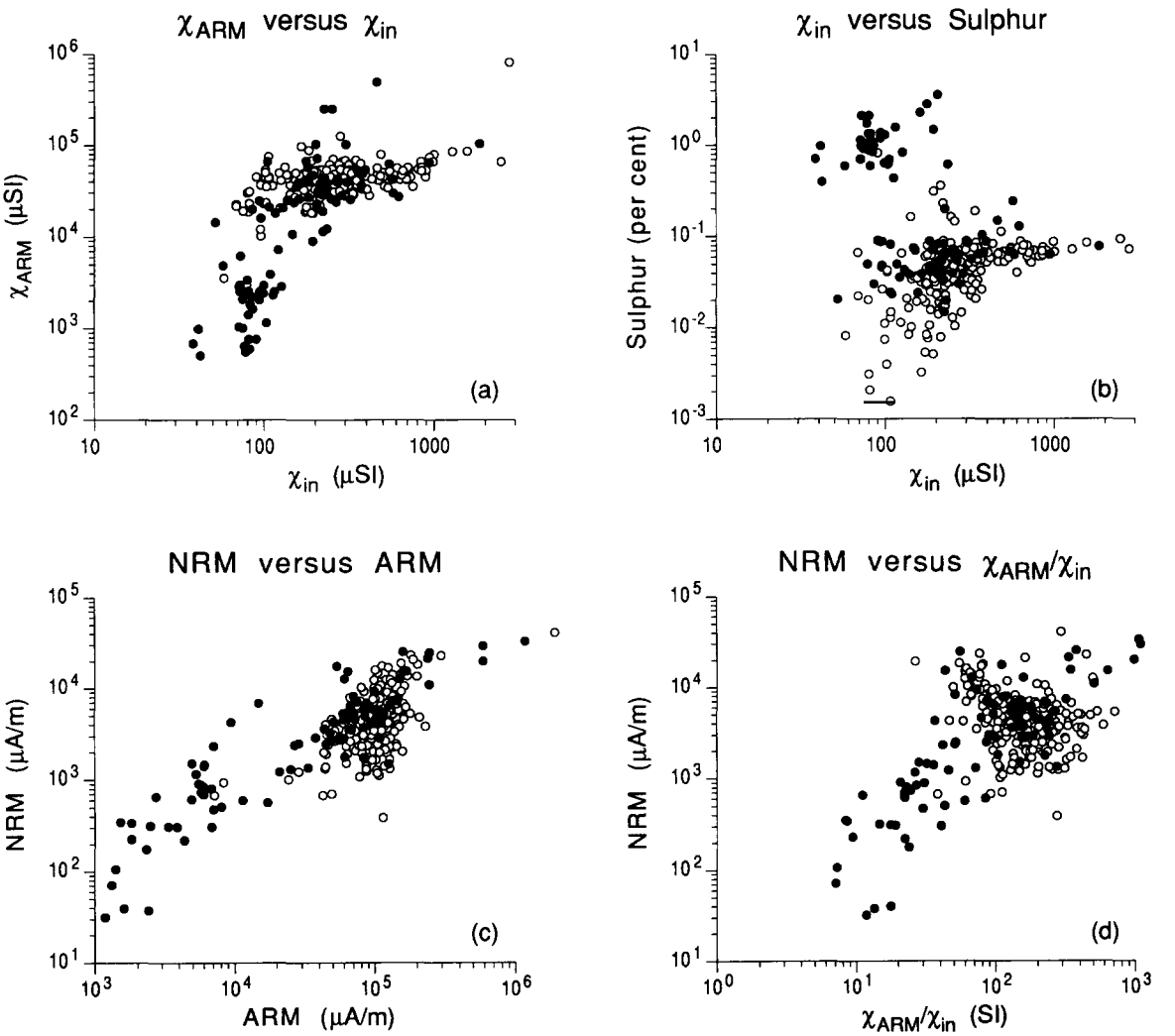

Fig. 4. Scattergrams of (a) χ_{ARM} vs. χ_{in}; (b) sulphur vs. χ_{in}; (c) NRM vs. ARM; (d) NRM vs. χ_{ARM}/χ_{in}. Full circles denote grey-coloured samples and samples from sapropelitic layers, open circles beige- and white-coloured samples. The beige- and white-coloured samples show distinctly less variation than the others.

appeared to be best expressed in an eight-cluster model (cf. Table 1).

Models with six or less clusters did not have sufficiently homogeneous clusters. Fine diagenetic features are not yet expressed in the cluster centres. From seven clusters upwards the composition of each cluster is rather homogeneous. Diagenetic features already emerge as distinct and interpretable clusters. Separate clusters with high χ_{in} and ARM, high S, high Ba, and high Mn can be distinguished. The main difference between the seven- and eight-cluster models is a better division with regard to the carbonate content of the samples, yielding a better grouping in the NLM plot (Fig. 5) for the eight-cluster model. Therefore, the (heuristically determined) eight-cluster model is preferred. Repeated runs indicate that solutions with nine or more clusters

were not stable with regard to their cluster centres. This may indicate that at this point homogeneous groups are split; this splitting may well be random. The robustness of the adopted model was tested by (1) leaving out Mn from the variable list, (2) division of S, Mn and Ba by Al, and (3) using different starting configurations for the iterative procedure. The subsequent reruns of the FCM program always led to similar cluster models with essentially the same samples.

The fuzzy *c*-means cluster centres and the geometric means of the so-called defuzzified clusters (with the cases forced completely into one cluster with the highest membership) are given in Table 1. The fuzzy cluster centres are less extreme, because they are based on the weighted contribution of all cases and better express the gradual character.

The clusters can be divided into two categories: one expressing mainly lithological features (clusters 1, 5, 7 and 8) and the other expressing mainly diagenesis (clusters 2, 3, 4 and 6) (cf. Fig. 6). The sequence of the clusters is arbitrary and has no statistical meaning. They are sorted in Table 1 according to their $CaCO_3$ content. In the following, we discuss the interpretation of each cluster, starting with the most obvious ones.

Dissolution and precipitation category

Cluster 4. Cluster 4 is marked by high S and very low ARM values. Under anoxic conditions, characterised by sulphate reduction, extensive dissolution of iron oxides has occurred, resulting in a very low ARM. Also χ_{in} is low, though less extreme because it is dominated by the paramagnetic contribution of clay minerals and the diamagnetic contribution of feldspars, quartz and carbonate. Cluster 4 samples are typically found in grey-coloured samples, usually below sapropelitic layers and occasionally above these layers.

Table 1
Cluster centres—ARM (mA m^{-1}), χ_{in} (μSI), $CaCO_3$ (%), Mn (ppm), Ba (ppm), S (ppm)

Variable	Fuzzy c-means cluster centres							
	1	2	3	4	5	6	7	8
χ_{in}	330	674	248	84	241	189	194	118
ARM	95.4	126	74.1	4.3	97.0	91.5	98.2	77.0
$CaCO_3$	27.2	30.9	32.5	33.8	37.5	42.3	53.4	70.2
Mn	750	1135	1390	920	860	1300	1225	1625
Ba	225	240	210	225	185	520	135	85
S	650	680	540	9270	470	960	260	80
Variable	Geometric means of the defuzzified clusters							
	1	2	3	4	5	6	7	8
χ_{in}	327	742	254	79.1	229	195	184	110
χ_{in} (CFB)	417	1008	350	119	346	315	364	336
ARM	94.8	142	74.0	4.01	90.8	110	92.1	74.8
ARM (CFB)	121	193	102	6.01	137	178	182	229
$CaCO_3$	26.1	30.7	31.9	35.3	38.3	41.0	53.8	71.4
Mn	720	1100	1430	995	835	1265	1295	1595
Ba	235	235	210	225	180	550	185	85
Ba (CFB)	300	320	290	335	275	890	270	260
S	650	680	550	8025	475	1515	260	80
S (CFB)	830	930	760	12050	700	2440	510	220
N	42 (9)	34 (6)	46 (6)	31 (0)	50 (5)	20 (3)	46 (10)	26 (3)

CFB indicates the geometric mean value for each cluster calculated on a carbonate-free basis, i.e. the contribution of $CaCO_3$ to the respective parameter is set to zero. This is not meaningful for Mn, because this element is correlated to $CaCO_3$ (a major part of the Mn is sorbed on to $CaCO_3$). Also, a small error is made for χ_{in} because χ_{in} for $CaCO_3$ is not zero, but slightly negative. In the number (*N*) of cases row, values between parentheses denote the number of intermediate cases (with a significant membership to more than one cluster) included in the defuzzified geometric means.

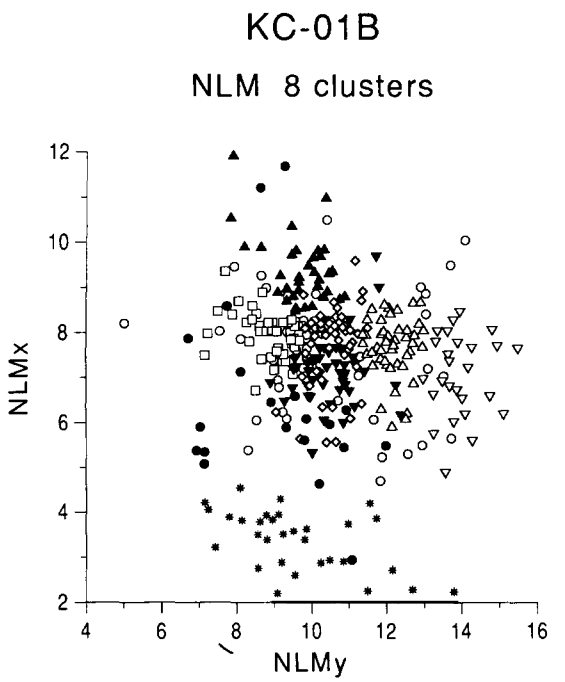

Fig. 5. The outcome of the non-linear mapping (NLM) after 100 iterations. The NLM axes have no physical meaning; to illustrate this (x, y) pairs are shown as (y, x) pairs. The lithology-category clusters are indicated with open symbols (cluster 1, squares; cluster 5, diamonds; cluster 7, triangles; cluster 8, inverted triangles) and the diagenesis-category clusters with full symbols (cluster 2, triangles; cluster 3, inverted triangles; cluster 4, asterisks; cluster 6, circles). Samples with no dominant membership of a single cluster are indicated with open circles. In general, observed grouping corresponds well with the grouping inferred from FCM; only cluster 6 (high Ba) is not tightly grouped. Apparently, high Ba-content samples can have quite differing compositions.

This can be explained by the extra duration available for dissolution processes created by the deposition of the severely anoxic sapropelitic layer on top of cluster 4 samples.

Cluster 6. This cluster is characterized by high Ba values. Some samples also have a high S content. Samples come either from a sapropelitic layer itself or are intimately associated with it. ARM values are more or less average values, possibly related to magnetite created by sulphate-reducing bacteria (Sakaguchi et al., 1993). Below the sapropelitic layers, however, the amount of organic material is considerably decreased, so in these intervals conditions are less favourable for these bacteria. As a consequence, there will be no or hardly any magnetite formed.

Cluster 2. Samples of cluster 2 are characterised by high ARM, fairly high Mn and high χ_{in}. A Mn content of 600–800 ppm would be normal for the carbonate percentages of cluster 2 samples (see Van Hoof et al., 1993), where we find a cluster centre value of 1135 ppm. Upon gradually changing redox conditions, Fe may remain mobile because the iron reduction zone is between suboxic and anoxic conditions (Froelich et al., 1979). It migrates and precipitates upon reaching more oxic (still suboxic) conditions, likely as magnetite because of the high ARM values. The high NRM values in this cluster are undoubtedly of CRM origin. Magnetite, formed by an oxidation reaction with green rust as intermediate phase, has experimentally been shown to carry a CRM (Pick and Tauxe, 1991; Dekkers et al., unpublished data). Quite a number of cluster 2 samples have an olive-greenish coloured tan.

Cluster 3. Cluster 3 samples are characterised by minor dissolution because of their comparatively low ARM and χ_{in} values, although not as low as those of cluster 4 samples. ARM and χ_{in} are still low, if calculated on a carbonate-free basis (CFB, Table 1). The relatively high Mn values in cluster 3 (in relation to its $CaCO_3$ content) indicate precipitation of Mn-(oxy)hydroxides, pointing to oxic–suboxic conditions. A possible explanation for this cluster is that conditions were formerly anoxic leading to mild magnetite dissolution, and that a later progressive oxidation front has stopped this dissolution process. Samples belonging to cluster 3 have no direct association to a sapropelitic layer and are mostly grey-coloured in the lower half of the core, or olive-greenish coloured in the upper part of the core.

Lithology category

Clusters 1, 5, 7 and 8. These clusters likely represent depositional conditions, only their $CaCO_3$ content differs. Sulphur and Ba values are low and indicate oxic to suboxic conditions, while the Mn content correlates well with the $CaCO_3$ content. The ARM values of the fuzzy

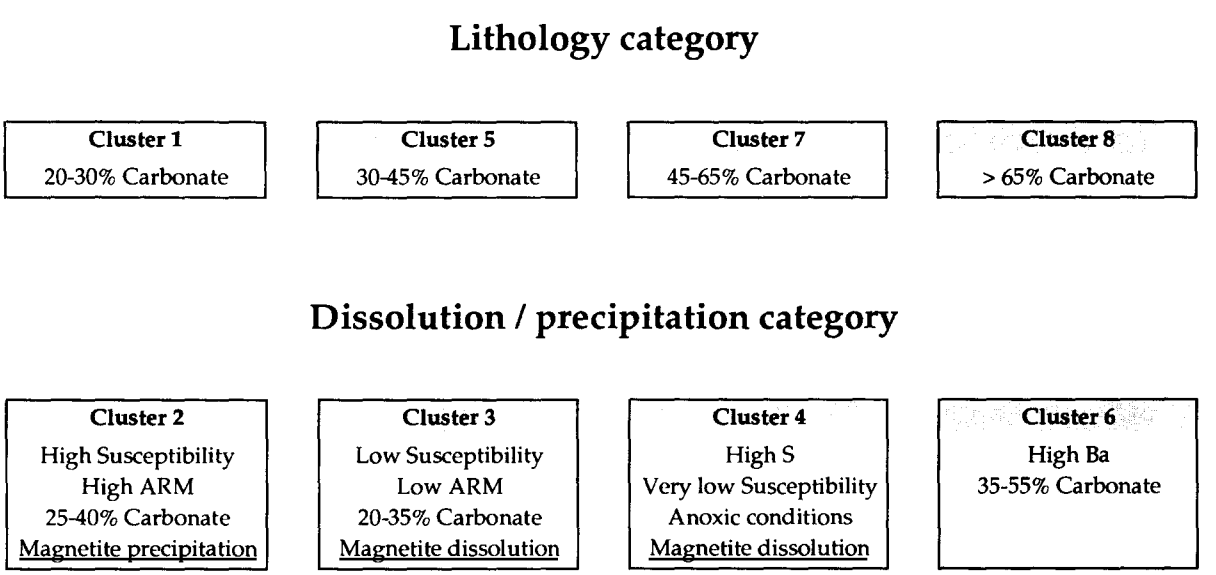

Fig. 6. Schematised properties of the clusters in the eight-cluster model.

cluster centres are similar for these clusters, as are CFB Ba and CFB χ_{in} values (Table 1). One should bear in mind two factors when comparing the CFB values.

(1) For this correction, in the calculation of the Ca content to $CaCO_3$, a constant 2% non-carbonate Ca value was assumed. In reality, this value may vary slightly, which may lead to some error for high $CaCO_3$ contents.

(2) The CFB correction assumes zero susceptibility for $CaCO_3$ which may lead to a noticeable underestimate of χ_{in} when dealing with high $CaCO_3$ contents, like in cluster 8. Samples belonging to cluster 8 with the highest $CaCO_3$ content are the white-coloured ones (very pale-beige and light-grey shades included). Consequently, they have the lowest χ_{in} and ARM.

All samples of clusters 7 and 8 occur below 15 m subbottom depth, with the exception of one sample (intermediate between clusters 7 and 8). Also cluster 5 samples occur predominantly in this interval. Samples of clusters 1, 5, 7 and 8 have preserved depositional conditions to a large extent. Despite the dominant lithological character of these clusters, incipient diagenesis may be suspected in some cases. This will be discussed in Section 5.4.

5. Discussion

5.1. Genetic relationships between clusters

The lithology category clusters (1, 5, 7 and 8) are not genetically related. The dissolution and precipitation category clusters (2, 3, 4 and 6) expressing diagenetic features, however, are genetically related, because the dissolved iron migrates and precipitates elsewhere, depending on the physico-chemical conditions. Cluster 4 and cluster 6 are closely related. The reservoir of organic matter in the sapropelitic layers has caused extensive sulphate reduction. The reduction front has moved outward from the sapropelitic layers giving rise to widespread dissolution of iron oxides. This results in cluster 4 samples. The cluster 4 zone is often particularly well developed below sapropelitic layers because of the longer duration available (downward migration already starts upon formation of the sapropelitic layer itself). The dissolved iron oxides will precipitate again upon reaching more oxic conditions. Therefore, the cluster 4 samples are usually bordered either by cluster 3 samples (mild dissolution) or by cluster 2 samples (precipitation), depending on the gradient in redox-conditions.

Samples belonging to the lithology-category clusters adjacent to samples of dissolution/precipitation-category clusters, often have distinctly high or low ARM/χ_{in} ratios when compared with geometric means for the respective clusters. Samples with high or low ARM/χ_{in} ratios having a reversed primary NRM direction occur usually in parts of the core where NRM demagnetisation revealed a partial overprint by a low-coercivity normal component (Langereis et al., 1994).

5.2. Visualisation of trends in bivariate plots

The interpretative value of a NLM plot (Fig. 5) is limited, because the axes have no 'physical' meaning. For interpretative purposes, bivariate

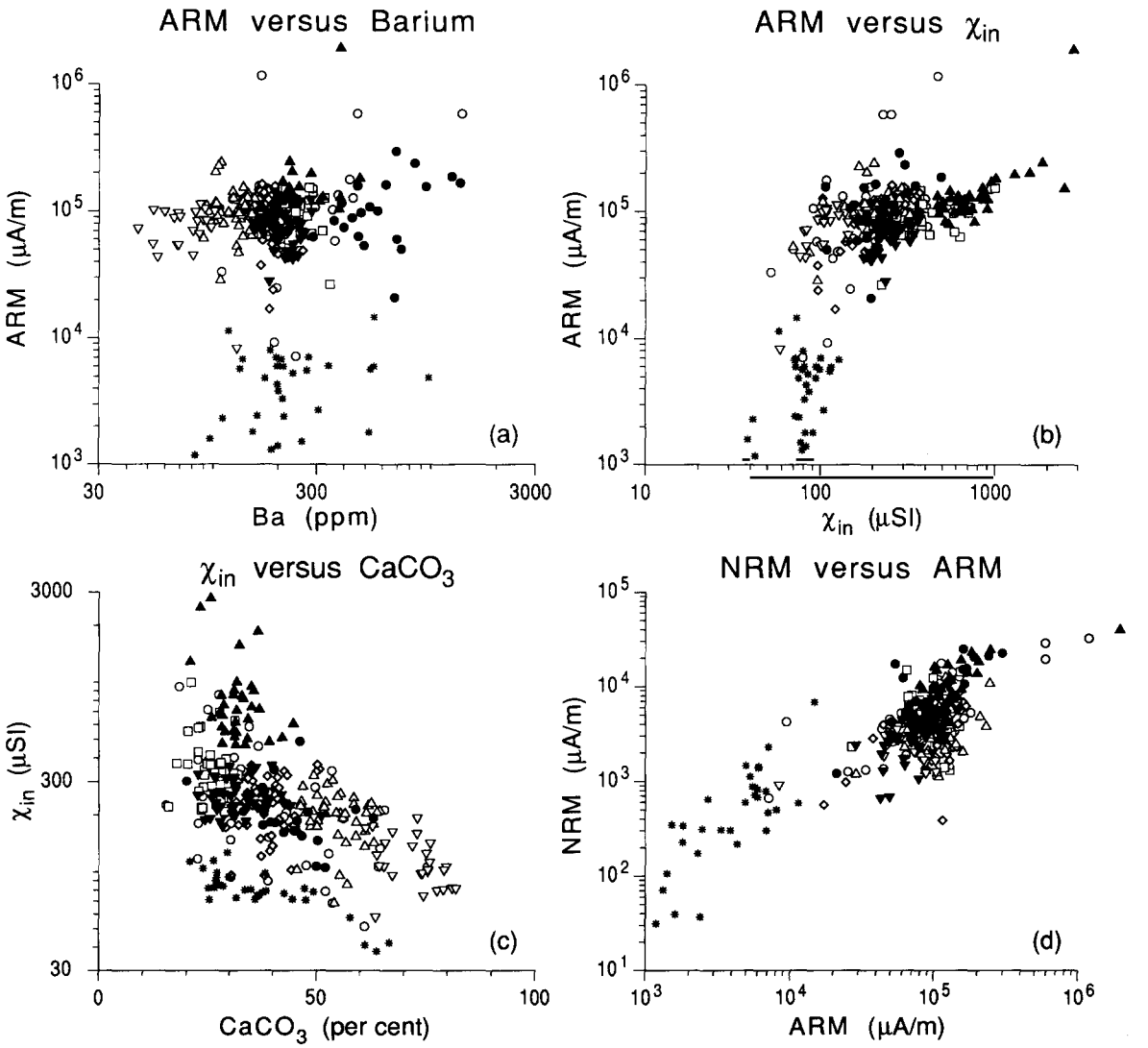

Fig. 7. Scattergrams with samples labelled according to their clusters: (a) Ba vs. ARM; (b) ARM vs. χ_{in}; (c) χ_{in} vs. $CaCO_3$; (d) NRM vs. ARM. For the cluster labelling the reader is referred to the caption of Fig. 5. Samples with no dominant membership of a single cluster are labelled with open circles.

plots and labelling of cluster divisions are more useful. A plot of the ARM intensity vs. Ba content (Fig. 7a) shows that clusters 4 (low ARM) and 6 (high Ba) — obvious diagenesis clusters — are separated from the main body of samples. Fig. 7(b), showing ARM intensity vs. χ_{in}, shows two groups which were already emerging from Fig. 4(a). Cluster 4 samples form one group (grey lithology). The behaviour of the other group in Fig. 4(a) (beige + white) can now be depicted in more detail with the help of the cluster labelling. Samples from the lithology category clusters (8, 7, 5 and 1) form the main body of this group. Cluster 2 samples, where precipitation is interpreted to occur, plot on the high end of this group, while cluster 3 samples (mild dissolution) appear in the middle of the group but mainly on the lower side. The dispersion of cluster 6 samples is considerable: since they do not show up as a distinct group, the diagenetic influence may be overlooked if one uses only the χ_{in} vs. ARM plot. Some cluster 1 samples also plot in the cluster 2 extension, and they appear to have deviating ARM/χ_{in} values (high or low). Fig. 7(c) shows χ_{in} vs. $CaCO_3$. Samples from clusters 1, 5, 7 and 8 form a band of decreasing χ_{in} with increasing $CaCO_3$ content, concurring with an increase in diamagnetic $CaCO_3$ and a corresponding decrease in paramagnetic clay content. Cluster 4 samples (extensive dissolution) plot as a group separated from the general band. Cluster 3 samples (mild dissolution) mainly plot on the lower side of the general band, like most of the cluster 6 samples (high Ba). Cluster 2 samples (precipitation) are clearly above the general band, though not distinctly separate. On the other hand, some samples of the lithology-category clusters 5, 7 and 8, however, plot below the general band. This is may be an indication that still some dissolution has taken place in these samples. Their $CaCO_3$ content apparently still dominates and classifies them in clusters 5, 7 or 8. Within these clusters, however, they plot away from the main body of the other samples. This illustrates that it is very useful to visualise data in different ways. The NRM vs. ARM plot is shown in Fig. 7(d). The lithology-category clusters plot in a very restricted area. The precipitation and mild dissolution clusters (2 and 3), however, show a large overlap with this area.

The cluster division also suggests the following. The palaeomagnetic analysis (see Fig. 1) revealed that the sedimentation rate in the top part of the Matuyama chron is considerably lower than in the Brunhes chron (Langereis et al., 1994). Almost all samples in this Matuyama interval belong to clusters 5, 7 and 8, i.e. they have an intermediate to high $CaCO_3$ content. If carbonate represents primary production, then a low terrigenous input would yield a $CaCO_3$-rich sediment with a low sedimentation rate, provided biogenic $CaCO_3$ production remains more or less constant (Van Os et al., 1993). Independent estimates of terrigenetic input are needed to test whether the terrigenous dilution is indeed much less in this interval which seems to be characterised by a shift to more glacial conditions (Ruddiman et al., 1989) and, hence, a drier climate.

5.3. Cluster characteristics of the observed short reversed geomagnetic events in the Brunhes

The samples from the three observed short reversed periods in the Brunhes are all allocated to clusters expressing lithology. CR1 (319 ka) and CR3 (552 ka) are classed in cluster 1 and CR2 (497 ka) in cluster 5. The samples adjacent to the reversed sample also express dominant lithology for the three cases. The sample from CR3 may express some precipitation because of its high ARM/χ_{in} value for cluster 1 samples (see Section 5.4). The reversed samples have recorded a reversed geomagnetic field for that (short) period. In all three samples, however, coercivity overlap between the characteristic and secondary directions precludes a determination of the intensity of the characteristic remanent magnetization component.

5.4. Rock magnetic criteria of sample selection for relative palaeointensity determination

Rock magnetic criteria for selection of samples for relative palaeointensity determination were first established by King et al. (1983). These include: (1) the NRM must reside in magnetite or

low Ti-magnetite of PSD grain size, (2) the magnetite concentration should not vary by more than a factor 20–30, and (3) the normaliser should mimic the NRM as much as possible. It is generally believed that ARM is best suited, although occasionally the use of IRM or χ_{in} as normaliser has been shown to be justifiable (Tauxe and Wu, 1990). Tauxe and Valet (1989) point out that the rock magnetic criteria are minimum criteria only and there can be additional, subtle factors like sediment flux and bioturbation activity. They emphasise the need for multiple records, preferably from varying (sedimentary) regimes. Tauxe and Wu (1990) argue that to establish a reliable palaeointensity record, there must be no coherence between normalised intensity and lithological parameters. Meynadier et al. (1992) take as an additional constraint that the ARM/χ_{in} values be less than 2.5 times the average core value to minimise grain-size variations which bias the ARM normaliser. Varying grain size may cause differences in statistical alignment by the (varying) geomagnetic field and, hence, in the efficiency of NRM acquisition (Meynadier et al., 1992). All these criteria, however, implicitly assume that the NRM is of PDRM origin and, once locked-in, is preserved.

With the multivariate analysis, the diagenetic impact can be assessed on each sample individually. The NRM signal is likely to be distorted in samples belonging to the diagenesis-category clusters. This may also be the case for 'intermediate' samples with at least a significant membership of one of these clusters (in total 155 samples).

Thermomagnetic analysis (Fig. 3) hints at magnetite as the dominant remanence carrier in the KC-01B core. The expression of the Curie temperature is not pronounced because the ferromagnetic contribution in these sediment samples represents only a small fraction of the total magnetic signal. Thermomagnetic runs of more beige-coloured samples showed similar behaviour. The presence of sulphide in most grey samples precludes the establishment of any original magnetite by means of thermomagnetic runs.

Generally, ARM/χ_{in} is taken as being indicative of variations in magnetite grain size. This is correct if ARM as well as χ_{in} are determined by the ferrimagnetic phase, i.e. magnetite. When dealing with low χ_{in} values dominated by paramagnetism as in the present case, however, the ARM/χ_{in} ratio expresses variations in magnetite concentration rather than in grain size. For example, take a sample with an ARM of 10 mA m^{-1} and a χ_{in} of 100 μSI of which ca. 90% is caused by paramagnetism. If the amount of ferrimagnetic material, i.e. magnetite, with exactly the same grain size is increased ten times, the ARM value is approximately 70 mA m^{-1} (calculated from the data of Sugiura (1979)) while χ_{in} is 190 μSI. The ARM/χ_{in} ratio has increased from 100 to 368 without any change in grain size. Hence, in lithology-category clusters, minor precipitation may be recognised on the basis of high ARM/χ_{in} values, and consequently also minor dissolution on the basis of distinctly low ARM/χ_{in} values. The following arbitrary procedure is adopted. A log–normal distribution is assumed for the ARM/χ_{in} values in each lithology-category cluster. In nature, trace constituents like the magnetite concentration in our case, are quite often log–normally distributed. Subsequently, for each individual lithology-category cluster, ARM/χ_{in} values larger than the antilog of the geometric mean plus one standard deviation are taken as being indicative of precipitation. Similarly, ARM/χ_{in} values smaller than the antilog of the geometric mean minus one standard deviation indicate dissolution. In this way, minor dispersion of ARM/χ_{in} (within each homogeneous cluster) is ascribed to variations in lithology, while more extreme dispersion is taken to indicate incipient dissolution or precipitation. Fig. 8 shows the position of samples with these high or low ARM/χ_{in} values in a χ_{in} vs. $CaCO_3$ plot. A considerable number of the samples are indeed located in areas occupied by diagenesis-category clusters (shaded areas). This standardisation of the ARM/χ_{in} ratio in lithology-category clusters identifies 45 samples with incipient dissolution or precipitation. The lines in Fig. 8 are calculated χ_{in}-curves for mixtures of calcite (taken as average for the diamagnetic contribution) and illite (taken as average for the paramagnetic contribution; values taken from Collinson (1983)) with a

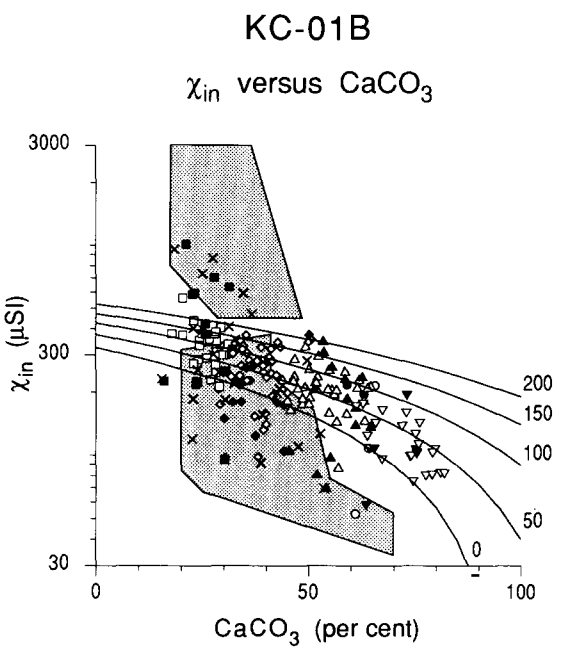

Fig. 8. The outcome of the ARM/χ_{in} standardisation procedure for the lithology-category clusters visualised in a χ_{in} vs. $CaCO_3$ plot. Lines refer to the behaviour of χ_{in} calculated for calcite/illite mixtures with a constant ferromagnetic contribution of 0, 50, 100, 150 and 200 μSI (see text). The shaded areas represent the diagenesis-category clusters 2, 3, 4 and 6. Samples of the lithology-category clusters are shown individually. Squares refer to samples of cluster 1, diamonds to those of cluster 5, triangles to those of cluster 7 and inverted triangles to those of cluster 8. For each cluster, filled symbols have a either ARM/χ_{in} value above the geometric mean plus the antilog of one standard deviation, or a ARM/χ_{in} value below the geometric mean minus the antilog of one standard deviation. In this way, the ARM/χ_{in} distribution is normalised to each (homogeneous) cluster separately. Also shown is the behaviour of the samples with no dominant membership of a single cluster: crosses refer to samples with a significant membership of at least one diagenesis-category cluster, open circles are intermediate between two lithology-category clusters.

constant ferromagnetic contribution to χ_{in} of 0, 50, 100, 150 and 200 μSI. The observed variations in χ_{in} for a similar $CaCO_3$ content are explained through minute variations in the magnetite content rather than by invoking fairly large changes in the paramagnetic contribution. The latter would imply distinct changes in composition of the detrital input which is unlikely for the deposition area.

In Fig. 2, the NRM/ARM values of the lithology-category samples are shown with open circles, the samples with deviating ARM/χ_{in} values with star symbols, and the samples which are influenced by diagenesis with full circles. The high NRM/ARM values close to sapropelitic layers are related to diagenetic phenomena rather than to geomagnetic field features. In this respect, it is noteworthy that the Blake event in the Mediterranean is reported immediately above sapropelitic layer S5 (Ryan, 1972; Tucholka et al., 1987; Tric et al., 1991). In the KC-01B core, the sample directly above sapropelitic layer S5 expresses minor precipitation (intermediate between clusters 2 and 1), while the next three samples all express precipitation (cluster 2). The ongoing diagenesis likely obliterated the preservation of the Blake event in the KC-01B core by recording the later (normal) field by magnetite precipitation. The expression of diagenesis can spatially be quite variable. It is hardly conceivable, however, that the Mediterranean Blake recordings are not influenced by diagenetic phenomena, given their very close association with sapropelitic layer S5.

This study shows that diagenesis is profound in the KC-01B piston core. The diagenetic influence appears to be most prominent for low $CaCO_3$ percentages. The diagenetic influence on samples should preferably be assessed on a per sample basis; it is not restricted to a certain time interval or distinct lithology. Furthermore, diagenesis is not restricted to the direct vicinity of sapropelitic layers which are only the most visible expression of anoxic conditions. The most intense diagenesis, however, is associated with these layers. One could argue that the occurrence of sapropelitic layers makes this core a special case. The Mediterranean Sea is often considered as a marginal basin displaying strong astronomically forced climatic effects. In extreme anoxic conditions, diagenetic processes are more intense. It must be realised, however, that redox-induced precipitation fronts have also been reported in open ocean conditions, especially where turbidites are involved (e.g. Nares Abyssal Plane, de

Lange (1986); Madeira Abyssal Plain, Van Os et al., 1994). Also, climatically induced variations in organic carbon fluxes may lead to such non-steady-state diagenesis in deep-sea sediments (e.g. Finney et al., 1988). Finally, the study by Nowaczyk (1991) shows a varying number of preserved reversed geomagnetic events during the past 500 kyr in open ocean conditions, suggesting the occurrence of diagenetic phenomena.

6. Conclusions

This study shows the merits of the combination of fuzzy *c*-means cluster (FCM) analysis and non-linear mapping (NLM) to identify the diagenetic influence on a per sample basis by using a combination of geochemical ($CaCO_3$, S, Ba, Mn) and rock magnetic variables (ARM, χ_{in}). An eight-cluster model was derived with clusters belonging to two categories: one expressing mainly diagenetic phenomena, i.e. dissolution and precipitation, and the other mainly expressing primary depositional conditions. With FCM and NLM, diagenesis can be detected independently of sediment colour which makes it more informative than rather rigid analyses based on sediment colour tied to lithology alone. The recognition of dissolution and precipitation is pertinent to a meaningful relative palaeointensity analysis. Ongoing diagenesis may obliterate the preservation of short geomagnetic events, and is likely the reason for the non-occurrence of the Blake event in this core. The three short geomagnetic events which are preserved in the core are all in clusters with dominant lithological features.

Acknowledgements

This study was carried out in the framework of the Marflux project of the MAST1 programme of the European Community. P.J. Verplak and H.J. Meijer performed the majority of the magnetic measurements. MJD acknowledges the Royal Netherlands Academy of Sciences and Arts (KNAW) for support in the form of a fellowship. The comments of two anonymous referees are appreciated.

References

Bezdek, C.J., 1981. Pattern Recognition with Fuzzy Objective Function Algorithms. Plenum Press, New York.

Bloemendal, J., King, J.W., Hall, F.R. and Doh, S.-J., 1992. Rock magnetism of Late Neogene and Pleistocene deep-sea sediments: Relationship to sediment source, diagenetic processes and sediment lithology. J. Geophys. Res., 97: 4361–4375.

Canfield, D.E., 1989. Reactive iron in marine sediments. Geochim. Cosmochim. Acta, 53: 619–632.

Canfield, D.E. and Berner, R.A., 1987. Dissolution and pyritisation of magnetite in anoxic sediments. Geochim. Cosmochim. Acta, 51: 645–659.

Champion, D.E., Lanphere, M.A. and Kuntz, M.A., 1988. Evidence for a new geomagnetic reversal from lava flows in Idaho: a discussion of short polarity reversals in the Brunhes and late Matuyama Polarity Chrons. J. Geophys. Res., 93: 11667–11680.

Collinson, D.W., 1983. Methods in Rock Magnetism and Palaeomagnetism — Techniques and Instrumentation. Chapman and Hall, London–New York.

de Lange, G.J., 1986. Early diagenetic reactions in interbedded pelagic and turbiditic sediments in the Nares Abyssal Plain (western North Atlantic): consequences for the composition of sediment and interstitial water. Geochim. Cosmochim. Acta, 50: 2543–2561.

Finney, B.P., Lyle, M.W. and Heath, G.R., 1988. Sedimentation at MANOP site H (eastern equatorial Pacific) over the past 4000000 years: climatically induced redox variations and their effects on transition metal cycling. Palaeoceanography, 3: 169–189.

Frapporti, G., Vriend, S.P. and van Gaans, P.F.M., 1993. Hydrogeochemistry of the shallow Dutch groundwater: Interpretation of the national groundwater quality monitoring network. Water. Resour. Res., 29: 2993–3004.

Froelich, P.N., Klinkhammer, G.P., Bender, M.L., Luedtke, N.A., Heath, G.R., Cullen, D., Dauphin, P., Hammond, D., Hartman, B. and Maynard, V., 1979. Early oxidation of organic matter in pelagic sediments of the eastern equatorial Atlantic: suboxic diagenesis. Geochim. Cosmochim. Acta, 43: 1075–1090.

Hilgen, F.J., 1991. Astronomical calibration of Gauss to Matuyama sapropels in the Mediterranean and implication for the Geomagnetic Polarity Time Scale. Earth Planet. Sci. Lett., 104: 226–244.

Hilgen, F.J. and Langereis, C.G., 1989. Periodicities of $CaCO_3$ cycles in the Pliocene of Sicily: discrepancies with the quasi-periods of the Earth's orbital cycles? Terra Nova, 1: 409–415.

Howarth, R.J. and Sinding-Larsen, R., 1983. Multivariate analysis. In: R.J. Howarth (Editor), Statistics and Data Analysis in Geochemical Prospecting — Handbook of Exploration Geochemistry, Vol. 2. Elsevier, Amsterdam, pp. 207–283.

Jöreskog, K.G., Klovan, J.E. and Reyment, R.A., 1976. Methods in Geomathematics 1 — Geological Factor Analysis. Elsevier, Amsterdam.

Karlin, R., 1990a. Magnetite diagenesis in marine sediments from the Oregon continental margin. J. Geophys. Res., 95: 4405–4419.

Karlin, R., 1990b. Magnetic mineral diagenesis in suboxic sediments at Bettis site W–N, NE Pacific Ocean. J. Geophys. Res., 95: 4421–4436.

Karlin, R. and Levi, S., 1985. Geochemical and sedimentological control of the magnetic properties of hemipelagic sediments. J. Geophys. Res., 90: 10373–10392.

King, J.W., Banerjee, S.K. and Marvin, J., 1983. A new rock-magnetic approach to selecting sediments for geomagnetic paleointensity studies: application to paleointensity for the last 4000 years. J. Geophys. Res., 88: 5911–5921.

Langereis, C.G., Dekkers, M.J., van Santvoort, P.J.M. and de Lange, G.J., 1994. Magnetostratigraphy and astronomical calibration of the last 1.1 Myr from a Central Mediterranean piston core and dating of short events in the Brunhes Chron. Earth Planet. Sci. Lett., in preparation.

Leslie, B.W., Lund, S.P. and Hammond, D.E., 1990. Rock magnetic evidence for the dissolution and authigenic growth of magnetic minerals within anoxic marine sediments of the California continental borderland. J. Geophys. Res., 95: 4437–4452.

Lovley, D.R. and Phillips, E.J.P., 1986. Availability of ferric iron for microbial reduction in bottom sediments of the fresh water tidal Potomac River. Appl. Environ. Microbiol., 52: 751–757.

Lovley, D.R., Stolz, J.F., Nord, Jr., G.L. and Phillips, E.J.P., 1987. Anaerobic production of magnetite by a dissimilatory iron-reducing microorganism. Nature, 330: 252–254.

Løvlie, R., 1989. Palaeomagnetic stratigraphy: a correlation method. Quat. Int., 1: 129–149.

Lyle, M., 1983. The brown-green color transition in marine sediments: a marker of the Fe(II)–Fe(II) redox boundary. Limnol. Oceanogr., 28: 1026–1033.

Meynadier, L., Valet, J.-P., Weeks, R., Shackleton, N.J. and Hagee, V.L., 1992. Relative geomagnetic intensity of the field during the last 140 ka. Earth Planet. Sci. Lett., 114: 39–57.

Middelburg, J.J. and de Lange, G.J., 1988. Geochemical characteristics as indicators of the provenance of Madeira abyssal plain turbidites. A statistical approach. Oceanol. Acta, 11: 1159–1164.

Mullender, T.A.T., van Velzen, A.J. and Dekkers, M.J., 1993. Continuous drift correction and separate identification of ferromagnetic and paramagnetic contributions in thermomagnetic runs. Geophys. J. Int., 114: 663–672.

Nowaczyk, N.R., 1991. High-resolution magnetostratigraphy of late-Quaternary Arctic marine sediments. Ph.D. Thesis, Alfred Wegener Institute for Polar and Marine Research, Bremerhaven.

Pick, T. and Tauxe, L., 1991. Chemical remanent magnetization in synthetic magnetite. J. Geophys. Res., 96: 9925–9936.

Ruddiman, W.F., Raymo, M.E., Martinson, D.G., Clement, B.M. and Backman, J., 1989. Pleistocene evolution: Northern hemisphere ice sheets and North Atlantic Ocean. Paleoceanography, 4: 353–412.

Ryan, W.B.F., 1972. Stratigraphy of late Quaternary sediments in the eastern Mediterranean. In: D.J. Stanley (Editor), The Mediterranean Sea. Dowden, Hutchinson & Ross, Stroudsburg, PA, pp. 149–169.

Sakaguchi, T., Burges, J.G. and Matsunaga, T., 1993. Magnetite formation by a sulphate-reducing bacterium. Nature, 365: 47–49.

Sammon, J.W., 1969. A non-linear mapping for data structure analysis. IEEE Trans. Comput., C18: 401–409.

Sammon, J.W., 1970. An optimal discriminant plane. IEEE Trans. Comput., C13: 826–829.

Sugiura, N., 1979. ARM, TRM and magnetic interactions: concentration dependence. Earth Planet. Sci. Lett., 42: 451–455.

Tauxe, L., 1993. Sedimentary records of relative paleointensity of the geomagnetic field: theory and practice. Rev. Geophys., 31: 319–354.

Tauxe, L. and Valet, J.-P., 1989. Relative paleointensity of the Earth's magnetic field from marine sedimentary records: a global perspective. Phys. Earth Planet. Inter., 56: 59–68.

Tauxe, L. and Wu, G., 1990. Normalised remanence in sediments of the western equatorial Pacific: Relative paleointensity of the geomagnetic field? J. Geophys. Res., 95: 12337–12350.

Tric, E., Laj, C., Valet, J.-P., Tucholka, P., Paterne, M. and Guichard, F., 1991. The Blake geomagnetic event: transition geometry, dynamical characteristics and geomagnetic significance. Earth Planet. Sci. Lett., 102: 1–13.

Tucholka, P., Fontugne, M., Guichard, F. and Paterne, M., 1987. The Blake magnetic polarity episode in cores from the Mediterranean Sea. Earth Planet. Sci. Lett., 86: 320–326.

Van Hoof, A.A.M., van Os, B.J.H., Rademakers, J.G., Langereis, C.G. and de Lange, G.J., 1993. A palaeomagnetic and geochemical record of the upper Cochiti reversal and two subsequent precessional cycles from Southern Sicily (Italy). Earth Planet. Sci. Lett., 117: 235–250.

Van Os, B.J.H., Middelburg, J.J. and de Lange, G.J., 1991. Possible diagenetic mobilisation of barium in sapropelitic sediment from the eastern Mediterranean. Mar. Geol., 100: 125–136.

Van Os, B.J.H., Visser, H.J., Middelburg, J.J. and de Lange, G.J., 1993. Occurrence of thin metal-rich layers in deep-sea sediments: A geochemical characterisation of copper remobilisation. Deep-Sea Res. Part I, Oceanographic Res. Papers, 40: 1713–1730.

Van Os, B.J.H., Lourens, L., Hilgen, F.J. and de Lange, G.J., 1994. The formation of Pliocene sapropels and carbonate cycles in the Mediterranean: dilution, diagenesis and productivity. Paleoceanography, in press.

Van Velzen, A.J., 1993. The influence of weathering on the magnetic properties of single domain magnetite in marine sediments. Terra Nova 5(Suppl. 1): 93 (conference abstract).

Vriend, S.P., van Gaans, P.F.M., Middelburg, J.J. and de Nijs, A., 1988. The application of fuzzy c-means cluster analysis and non-linear mapping to geochemical datasets: examples from Portugal. Appl Geochem., 3: 213–224.

Zadeh, L.A., 1965. Fuzzy sets. Inf. Control, 8: 338–353.